

Ongoing fragmentation of the subducting Cocos slab, Central America

Tu Xue¹, Diandian Peng², Kelly H. Liu¹, Jonathan Obrist-Farner¹, Marek Locmelis¹, Stephen S. Gao^{1,*}, and Lijun Liu^{2,*}

¹Geology and Geophysics Program, Missouri University of Science and Technology, Rolla, Missouri 65409, USA

²Department of Geology, University of Illinois at Urbana-Champaign, Champaign, Illinois 61801, USA

ABSTRACT

Fundamental to plate tectonics is the subduction of cold and mechanically strong oceanic plates. While the subducted plates are conventionally regarded to be impermeable to mantle flow and separate the mantle wedge and the slab region, isolated openings have been proposed. By combining new shear wave splitting measurements with results from geodynamic modeling and recent seismic tomography and geochemical observations, we show that the upper ~200 km of the Cocos slab in northern Central America is intensively fractured. The slab there is strong enough to produce typical arc volcanoes and Benioff Zone earthquakes but allows mantle flow to traverse from the slab region to the mantle wedge. Upwelling of hot slab mantle flow through the slab provides a viable explanation for the behind-the-volcanic-front volcanoes that are geochemically distinct from typical arc volcanoes, and for the puzzling high heat flow, high elevation, and low Bouguer gravity anomalies observed in northern Central America.

INTRODUCTION

The Cocos Plate is bounded by the East Pacific Rise on the west and the Galapagos spreading center to the south (Fig. 1). It was formed when the Farallon Plate broke into two pieces at ca. 23 Ma (Pardo and Suárez, 1995; Dougherty et al., 2012; Borgeaud et al., 2019). The Cocos Plate is subducting beneath the North American and Caribbean plates, and compared with most other regions with convergent plate boundary zones, northern Central America has several puzzling characteristics including anomalously high topography (Rogers et al., 2002), high heat flow (Blackwell et al., 1990), low Bouguer gravity anomalies (Fig. S1 in the Supplemental Material¹), and the presence of intraplate Cenozoic volcanoes in eastern Guatemala and western El Salvador (Fig. 1). A compilation of measurements from existing geochemical studies indicates that the trace element patterns normalized against the com-

position of the upper continental crust (Rudnick and Gao, 2003) within the volcanic front (VF) and behind the volcanic front (BVF) are notably different (Fig. 2A). The VF lavas display features commonly associated with hydrous magmas derived from a subducting slab, most notably distinct negative Nb and Ta anomalies (Baier et al., 2008). Conversely, the absence of distinct negative Nb and Ta anomalies in the BVF lavas suggests that the BVF lavas formed from partial melting of a protolith without significant water content. Another unusual feature of this area is the lack of deep-focus earthquakes and a large reduction in earthquake productivity in the depth range of ~100–200 km relative to the other subduction zones, including those in neighboring southern Mexico and southern Central America (Fig. 2B).

Mainly due to poor coverage by seismic stations and the resulting low resolution of seismic tomographic images, conflicting conclusions regarding the continuity and geometry of the Cocos slab have been reached by different tomography studies. Based on a global-scale P-wave velocity model, Rogers et al. (2002)

proposed the existence of an isolated opening (termed slab gap herein) in the depth range of 200–500 km that horizontally extends for ~900 km from southern Mexico to Honduras. They attributed the high elevation in the back-arc area to upwelling mantle flow through this slab gap. This model, however, is inconsistent with more recent tomographic images. A regional-scale full-waveform inversion study (Zhu et al., 2020) revealed a continuous Cocos slab extending from the surface to a depth of at least 1000 km. The same study also found that in the top 200 km, the velocity anomaly of the slab is significantly weaker than that in deeper sections of the slab (Fig. S2), consistent with the reduced seismicity around this depth (Fig. 2B). Additionally, at depths greater than 80 km, the dominant fast orientation of seismic anisotropy, which represents the mantle flow direction in the sublithospheric mantle, is different between the oceanic and continental sides (Zhu et al., 2020). Specifically, it is trench-perpendicular on the Cocos side and becomes east-west on the Caribbean side with a clear right-turn pattern (Fig. S3). By combining results from previous geophysical investigations with insights from new shear wave splitting and geodynamic modeling studies, we propose a new model invoking ongoing fragmentation of the subducting Cocos slab.

CONSTRAINTS ON THE MANTLE FLOW FIELDS FROM SHEAR WAVE SPLITTING ANALYSIS

In addition to seismic tomography data, numerous studies have demonstrated that the mantle flow system in the vicinity of a subducting slab can be delineated by analyzing shear wave splitting, the birefringence of shear waves when they travel through an anisotropic

Stephen S. Gao  <https://orcid.org/0000-0001-7530-7128>

*Corresponding authors: sgao@mst.edu; ljliu@illinois.edu

¹Supplemental Material. Figures S1–S5 (Bouguer gravity anomalies and focal mechanism solutions; cross section of tomographic images and anisotropy beneath Central America; isotropic S-wave speed anomalies and azimuthal anisotropy; azimuthal equidistant map showing event distributions; and shear wave splitting measurement examples); Table S1 (shear wave splitting measurements); and Table S2 (model parameters). Please visit <https://doi.org/10.1130/G51403.1> to access the supplemental material; contact editing@geosociety.org with any questions.

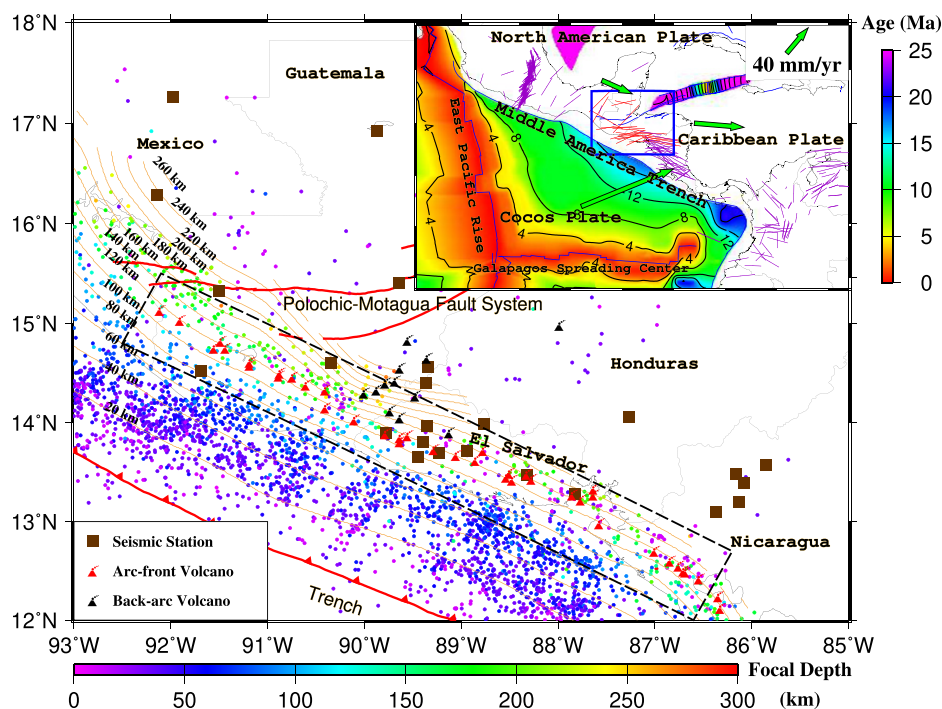


Figure 1. Tectonic setting of northern Central America. The colored dots represent the epicenters and focal depths of $\geq M4.5$ earthquakes that occurred between 1980 and 2022 CE. The yellow contour lines show the depths of the Cocos slab. The area outlined by the dashed black rectangle indicates the approximate extent of the proposed previous slab. The enclosed region outlined in blue in the inset map shows the study area, where the contour lines show the ocean floor ages. The purple and red lines represent results from previous and the present shear wave splitting studies, respectively (Russo and Silver, 1994; Piñero-Feliciangeli and Kendall, 2008; Abt et al., 2010; Masy et al., 2011; van Benthem et al., 2013; Porritt et al., 2014; Bernal-López et al., 2016; Idárraga-García et al., 2016; Castellanos et al., 2017). The orientations of the bars show the fast polarization orientation, and the length of the bars is proportional to the splitting time. Plate boundaries are from Bird (2003).

medium (Hess, 1964; Silver and Chan 1991; Long and Silver, 2009; Zhou et al., 2018; Kong et al., 2022). Relative to seismic tomography, shear wave splitting analysis (see Methods in the Supplemental Material) has a higher lateral and lower vertical resolution. In Nicaragua and adjacent areas, which are located to the southeast of the study area, the fast orientations from shear wave splitting analysis are largely trench-parallel and can be interpreted to reflect along-trench flow in the mantle wedge and beneath the slab (Abt et al., 2010). In contrast, the fast orientations in southern Mexico are dominantly trench-perpendicular and are interpreted as reflecting subduction-induced corner flow in the mantle wedge (Bernal-López et al., 2016) (Fig. 1), as widely observed in other subduction zones worldwide (Long and Silver, 2009).

Within our study area, however, the fast orientations from shear wave splitting analysis for the Caribbean Plate, overriding the Cocos slab, are neither trench-parallel nor trench-perpendicular, but oblique to it, and no systematic spatial variations in the splitting times are observed (Fig. 3). More intriguingly, observations at seismic stations located on the southwestern side of the volcanic arc show a clear dependence on the arriving azimuth of

the seismic waves (i.e., the back azimuth of the seismic events). In particular, the resulting fast orientations tend to be more perpendicular to the trench for ray paths arriving at the stations from the southwest, which sample the ocean side of the mantle, than those from other back azimuths. This pattern is consistent with a clockwise rotation of the inferred mantle flow directions that is also revealed by results from a full-waveform tomographic inversion (Zhu et al., 2020) (Fig. S3). Another notable feature is a sudden change in anisotropy orientations across the North American–Caribbean Plate boundaries, where results in the northern part are more trench-normal, which resembles typical corner flow. This implies an abnormal flow pattern below the Caribbean Plate in northern Central America.

NUMERICAL SIMULATION OF CENOZOIC COCOS SUBDUCTION

To quantitatively evaluate the subduction dynamics of the Cocos Plate, we performed numerical models with data-assimilation (Liu and Stegman, 2011) that satisfy the observed Cenozoic plate motion history and seafloor ages (see Methods in the Supplemental Material). Simulations starting no later than 40 Ma

produce similar present-day slab structures at <800 km depth. Our results from a case study that covers subduction since 45 Ma show that below the study area, the central portion of the Cocos slab experienced gradual shallowing since ca. 30 Ma while developing instabilities, and eventually developed a central slab tear along the slab hinge, toward the present (Fig. 4). The evolving slab geometry is characterized by multiple fold-like downwelling features with highly extended thin slab in between (Figs. 4D and 4E). The present slab geometry, with a thin slab segment above 200 km depth (Fig. 4B) and a deeper folded slab pile (Fig. 4E), matches the recent seismic tomographic results well (Fig. 4F).

The progressive dip angle reduction leading to the current fragmenting slab below the studied region reflects the sub-slab pressure accumulation over time: the finite width of the young (and weak) Cocos Plate allows the sub-slab pressure to be released around the northern and southern edges of the slab but not in the center. Consequently, the reduced slab dip angle is a result of the enhanced pressure gradient across the deformable slab below the western part of the Caribbean Plate. In addition, the differential trench motion (with the northern Cocos trench retreating faster than that south of the North America–Caribbean–Cocos triple junction since 30 Ma) further enhanced this north-south contrasting slab movement, facilitating slab flattening and deformation in the study region. Slab buckling with potential fracturing started to develop along the slab hinge at ca. 20 Ma between 86°W and 93°W (Figs. 4A and 4B), representing failure of the weak and young subducting plate due to sub-slab overpressure. This process coincides with the mid-Miocene ignimbrite flare-up event in Central America (Sigurdsson et al., 1997; Leckie et al., 2000) and is also similar to what occurred within the Farallon slab during the mid-Miocene, where the slab tear below Oregon and Nevada (USA) led to abrupt surface uplift, upwelling within the mantle wedge, and the development of the Columbia River flood basalts (Liu and Stegman, 2012). The observed high topography (Fig. 3) and low Bouguer gravity (Fig. S1) above the predicted slab gap in the study area further support this model result.

ONGOING FRAGMENTATION OF THE COCOS SLAB AND ITS GEODYNAMIC IMPLICATIONS

The recognition of a fragmenting Cocos slab that is permeable to mantle flow, i.e., a pervious slab, can reconcile multiple lines of seemingly contradictory observations. For example, seismic tomography has revealed a broken or significantly weakened upper-mantle slab (Rogers et al., 2002; Zhu et al., 2020). In contrast, the existence of intermediate-depth earthquakes

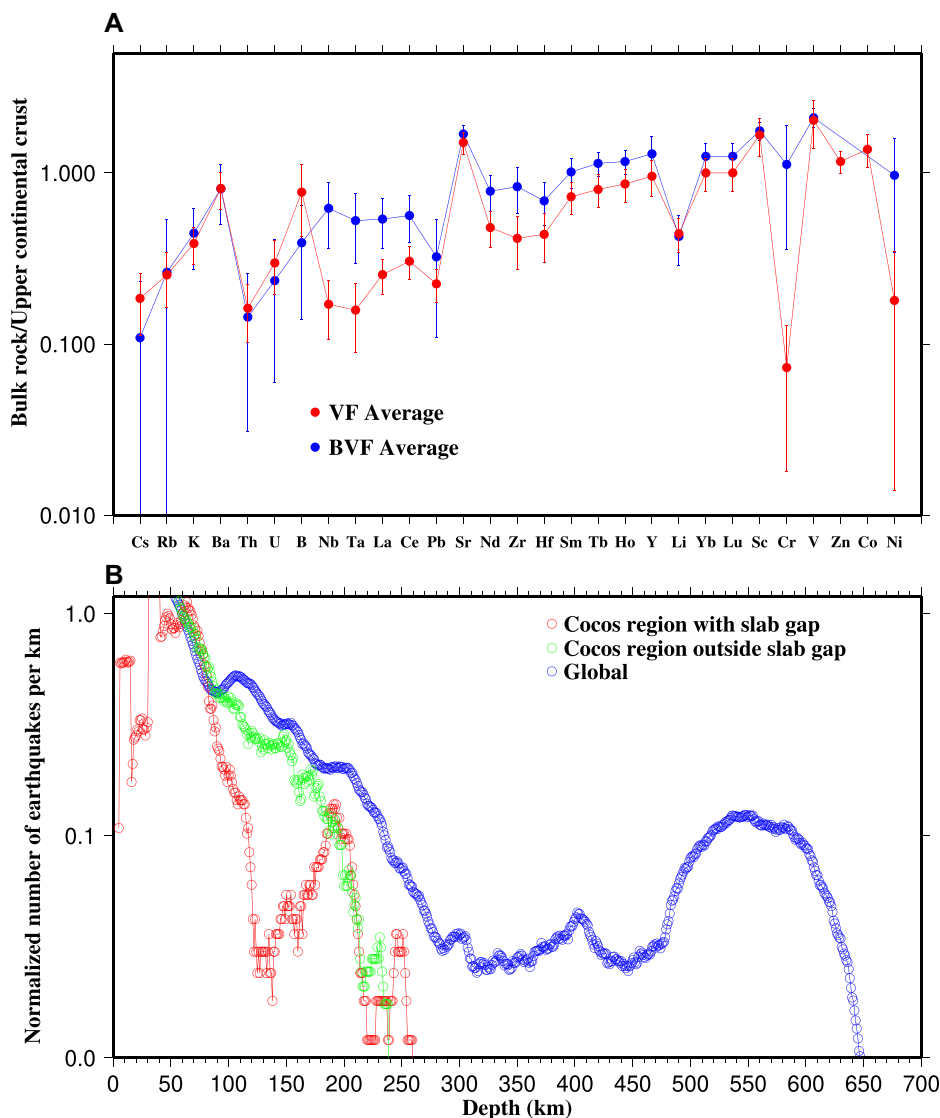


Figure 2. Chemical composition and earthquake distribution of the Cocos slab, Central America. (A) Elemental compositions of volcanic front (VF) and behind the volcanic front (BVF) samples normalized to the composition of the upper continental crust, after Rudnick and Gao (2003). The data shown were compiled from Walker et al. (1995, 2000, 2009), Carr et al. (2014), and Patino et al. (2000). Error bars represent one standard deviation. (B) Depth variation of the number of $\geq M4.0$ earthquakes that occurred between 2010 and 2022 CE in northern Central America from the slab gap region (red), from outside the slab gap region (green), and for all subduction zones on Earth (blue). Results are normalized by the corresponding value at 60 km depth.

and VF volcanoes is inconsistent with the existence of a typical slab gap, which is a hole in the slab that is incapable of generating earthquakes. According to our simulated current slab geometry (Fig. 4D), inferences of seismic anisotropy (Fig. 3), as well as the area of low Bouguer gravity anomalies (Fig. S1), the fragmented portion of the Cocos slab has an along-trench dimension of ~ 700 km, approximately between 86°W and 93°W . In our model, this slab fragmentation starts at ~ 60 km depth, immediately beneath the lithosphere of the overriding plate, as is confirmed by the observation that the anisotropy-indicated flow systems below ~ 80 km in the sub-slab region and the mantle

wedge show a high degree of continuity (Zhu et al., 2020) (Fig. S3). The maximum depth of the intensively fractured portion is ~ 200 km, as this is the depth of suddenly thickened slab thermal structure (Fig. 4E) and increased seismic velocity anomalies (Zhu et al., 2020) (Fig. 4F; Fig. S2). This gap also coincides with the area of anomalously low earthquake productivity (Fig. 2B).

The intensively fractured section of the Cocos slab above 200 km depth is mechanically weaker and warmer than a normal slab due to the strong internal deformation associated with ongoing fragmentation (Fig. 4). Consequently, this slab portion should have a

lower earthquake productivity (Fig. 2B). Both the reduced mechanical strength and higher temperature of the intensively fractured portion of the slab may also be responsible for the slightly positive velocity anomaly relative to the deeper portion, as revealed by seismic tomography (Zhu et al., 2020). This portion of the slab can still carry a sufficient amount of hydrous phases to produce the VF volcanoes. Meanwhile, the sub-slab mantle material, which is under enhanced dynamic pressure and has a higher temperature than that in the mantle wedge (Blackwell et al., 1990) (and is thus more buoyant), actively migrates upward through the tearing slab hinge to produce the higher-than-normal heat flow, anomalously high elevation (Fig. 3), low Bouguer gravity anomalies (Fig. S1), and the BVF volcanoes.

ACKNOWLEDGMENTS

The seismic data used in this study were obtained from the Incorporated Research Institutions for Seismology Data Management Center, Seattle, Washington, USA (<https://ds.iris.edu/ds/nodes/dmc/>). The original version of CitcomS is available at <https://geodynamics.org/> (see Supplemental Material). We thank Giovanni Camanni, Yu Jeffery Gu, an anonymous reviewer, and editor William Clyde for constructive reviews. This study was supported by the National Science Foundation (grants 1321656 to K. Liu, 1554554 to L. Liu, and 1830644 to K. Liu and S. Gao).

REFERENCES CITED

- Abt, D.L., Fischer, K.M., Abers, G.A., Protti, M., González, V., and Strauch, W., 2010, Constraints on upper mantle anisotropy surrounding the Cocos slab from $SK(K)S$ splitting: *Journal of Geophysical Research: Solid Earth*, v. 115, B06316, <https://doi.org/10.1029/2009JB006710>.
- Baier, J., Audéat, A., and Keppler, H., 2008, The origin of the negative niobium tantalum anomaly in subduction zone magmas: *Earth and Planetary Science Letters*, v. 267, p. 290–300, <https://doi.org/10.1016/j.epsl.2007.11.032>.
- Bernal-López, L.A., Garibaldi, B.R., Soto, G.L., Valenzuela, R.W., and Escudero, C.R., 2016, Seismic anisotropy and mantle flow driven by the Cocos slab under southern Mexico: *Pure and Applied Geophysics*, v. 173, p. 3373–3393, <https://doi.org/10.1007/s00024-015-1214-7>.
- Bird, P., 2003, An updated digital model of plate boundaries: *Geochemistry, Geophysics, Geosystems*, v. 4, 1027, <https://doi.org/10.1029/2001GC000252>.
- Blackwell, D.D., Steele, J.L., and Carter, L.C., 1990, Heat flow patterns of the North American continent: A discussion of the DNAG geothermal map of North America: DOE/EEGTP (U.S. Department of Energy Office of Energy Efficiency and Renewable Energy Geothermal Technologies Program) Technical Report, <https://doi.org/10.2172/896322>.
- Borgeaud, A.F., Kawai, K., and Geller, R.J., 2019, Three-dimensional S velocity structure of the mantle transition zone beneath Central America and the Gulf of Mexico inferred using waveform inversion: *Journal of Geophysical Research: Solid Earth*, v. 124, p. 9664–9681, <https://doi.org/10.1029/2018JB016924>.
- Carr, M.J., Feigenson, M.D., Bolge, L.L., Walker, J.A., and Gazel, E., 2014, RU_CAGeochem, a database and sample repository for Central American vol-

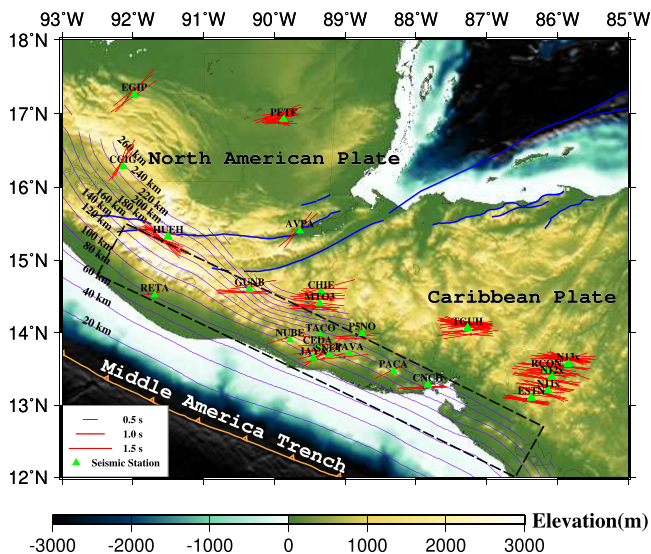


Figure 3. Results from shear wave splitting analysis. Individual splitting measurements (red bars) from this study are plotted at the seismic stations along the Cocos slab and above the ray-piercing points at 50 km depth. The area outlined by the dashed rectangle indicates the approximate extent of the proposed pervious slab. Blue lines are major faults.

canic rocks at Rutgers University: *Geoscience Data Journal*, v. 1, p. 43–48, <https://doi.org/10.1002/gdj3.10>.
Castellanos, J., Pérez-Campos, X., Valenzuela, R., Husker, A., and Ferrari, L., 2017, Crust and upper-mantle seismic anisotropy variations from the coast to inland in central and Southern Mexico: *Geophysical Journal International*,

v. 210, p. 360–374, <https://doi.org/10.1093/gji/ggx174>.
Dougherty, S.L., Clayton, R.W., and Helmberger, D.V., 2012, Seismic structure in central Mexico: Implications for fragmentation of the subducted Cocos plate: *Journal of Geophysical Research: Solid Earth*, v. 117, B09316, <https://doi.org/10.1029/2012JB009528>.

Hess, H.H., 1964, Seismic anisotropy of the uppermost mantle under oceans: *Nature*, v. 203, p. 629–631, <https://doi.org/10.1038/203629a0>.
Idárraga-García, J., Kendall, J.M., and Vargas, C.A., 2016, Shear wave anisotropy in northwestern South America and its link to the Caribbean and Nazca subduction geodynamics: *Geochemistry, Geophysics, Geosystems*, v. 17, p. 3655–3673, <https://doi.org/10.1002/2016GC006323>.
Kong, F., Gao, S.S., Liu, K.H., Fang, Y., Zhu, H., Stern, R.J., and Li, J., 2022, Metastable olivine within oceanic lithosphere in the uppermost lower mantle beneath the eastern United States: *Geology*, v. 50, p. 776–780, <https://doi.org/10.1130/G49879.1>.
Leckie, R.M., Sigurdsson, H., Acton, G.D., and Draper, G., eds., 2000, *Proceedings of the Ocean Drilling Program, Scientific results*, v. 165: College Station, Texas, Ocean Drilling Program, 236 p., <https://doi.org/10.2973/odp.proc.sr.165.2000>.
Liu, L., and Stegman, D.R., 2011, Segmentation of Farallon slab: *Earth and Planetary Science Letters*, v. 311, p. 1–10, <https://doi.org/10.1016/j.epsl.2011.09.027>.
Liu, L., and Stegman, D.R., 2012, Origin of Columbia River flood basalt controlled by propagating rupture of the Farallon slab: *Nature*, v. 482, p. 386–389, <https://doi.org/10.1038/nature10749>.
Long, M.D., and Silver, P.G., 2009, Mantle flow in subduction systems: The slab flow field and implications for mantle dynamics: *Journal of Geophysical Research: Solid*

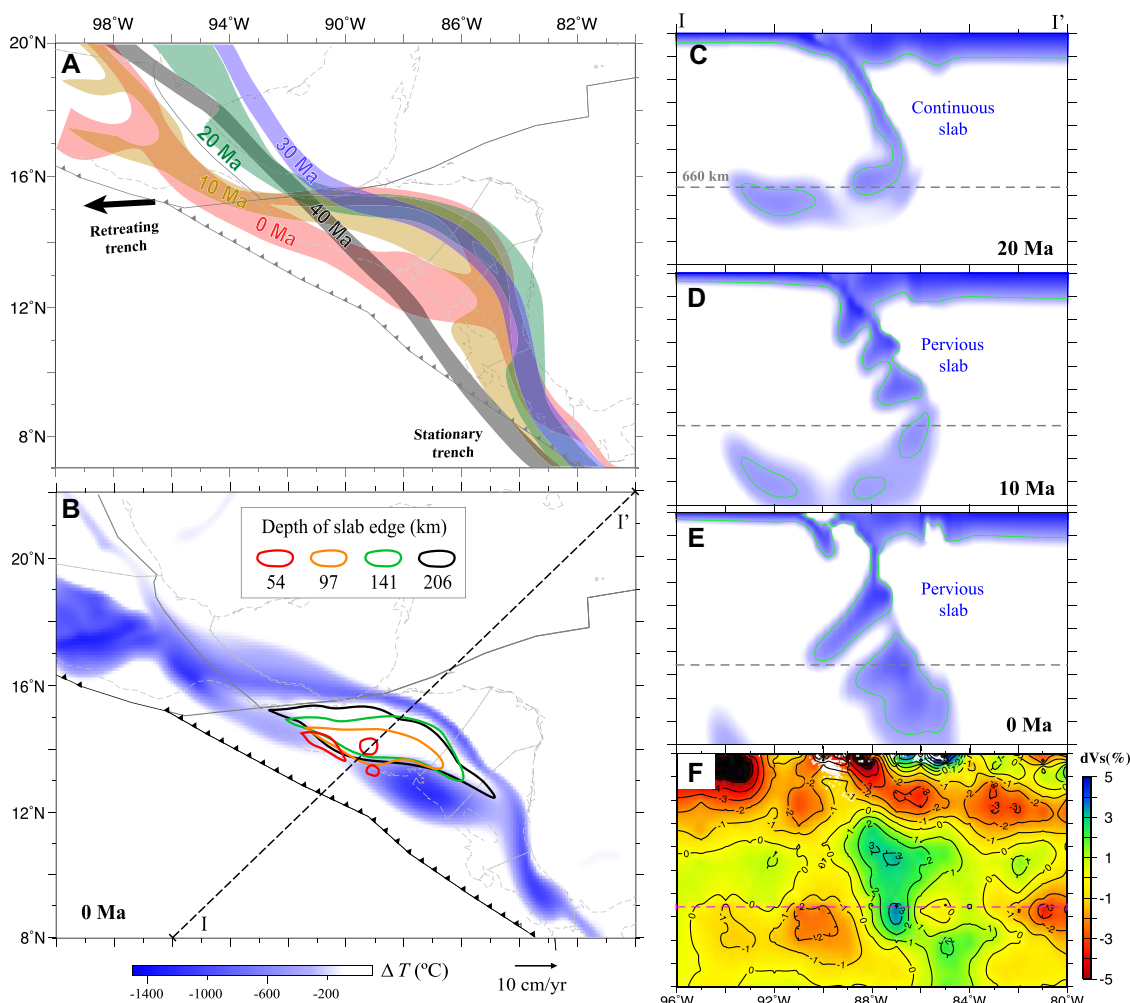


Figure 4. Modeled Cocos subduction and current slab geometry. (A) Map view of slab evolution at 160 km depth from 40 Ma to the present. Colored translucent patterns show slab interiors (400 °C colder than the ambient mantle). (B) Current slab geometry at 206 km depth, with color contours outlining the major slab gap at different depths. (C–E) Cross sectional view of subduction along I–I' shown in B, at different times. Green contours represent the –400 °C isotherm anomaly. (F) Seismic image of current slab structure along I–I' (see Zhu et al., 2020, and references therein). On the vertical axis of C–F, each tick mark represents 100 km in depth.

- Earth, v. 114, B10312, <https://doi.org/10.1029/2008JB006200>.
- Masy, J., Niu, F., Levander, A., and Schmitz, M., 2011, Mantle flow beneath northwestern Venezuela: Seismic evidence for a deep origin of the Mérida Andes: *Earth and Planetary Science Letters*, v. 305, p. 396–404, <https://doi.org/10.1016/j.epsl.2011.03.024>.
- Pardo, M., and Suárez, G., 1995, Shape of the subducted Rivera and Cocos plates in southern Mexico: Seismic and tectonic implications: *Journal of Geophysical Research: Solid Earth*, v. 100, p. 12,357–12,373, <https://doi.org/10.1029/95JB00919>.
- Patino, L.C., Carr, M.J., and Feigenson, M.D., 2000, Local and regional variations in Central American arc lavas controlled by variations in subducted sediment input: *Contributions to Mineralogy and Petrology*, v. 138, p. 265–283, <https://doi.org/10.1007/s004100050562>.
- Piñero-Feliciangeli, L.T., and Kendall, J.M., 2008, Sub-slab mantle flow parallel to the Caribbean plate boundaries: Inferences from SKS splitting: *Tectonophysics*, v. 462, p. 22–34, <https://doi.org/10.1016/j.tecto.2008.01.022>.
- Porritt, R.W., Becker, T.W., and Monsalve, G., 2014, Seismic anisotropy and slab dynamics from SKS splitting recorded in Colombia: *Geophysical Research Letters*, v. 41, p. 8775–8783, <https://doi.org/10.1002/2014GL061958>.
- Rogers, R.D., Kárasón, H., and van der Hilst, R.D., 2002, Epeirogenic uplift above a detached slab in northern Central America: *Geology*, v. 30, p. 1031–1034, [https://doi.org/10.1130/0091-7613\(2002\)030<1031:EUAADS>2.CO;2](https://doi.org/10.1130/0091-7613(2002)030<1031:EUAADS>2.CO;2).
- Rudnick, R.L., and Gao, S., 2003, Composition of the continental crust, in Holland, H.D., and Turekian, K.K., eds., *Treatise on Geochemistry* (volume 3): Amsterdam, Elsevier, p. 1–64, <https://doi.org/10.1016/B0-08-043751-6/03016-4>.
- Russo, R.M., and Silver, P.G., 1994, Trench-parallel flow beneath the Nazca plate from seismic anisotropy: *Science*, v. 263, p. 1105–1111, <https://doi.org/10.1126/science.263.5150.1105>.
- Sigurdsson, H., et al., 1997, *Proceedings of the Ocean Drilling Program, Initial reports*, v. 165: College Station, Texas, Ocean Drilling Program, 400 p., <https://doi.org/10.2973/odp.proc.ir.165.1997>.
- Silver, P.G., and Chan, W.W., 1991, Shear wave splitting and subcontinental mantle deformation: *Journal of Geophysical Research: Solid Earth*, v. 96, p. 16,429–16,454, <https://doi.org/10.1029/91JB00899>.
- van Benthem, S., Govers, R., Spakman, W., and Wortel, R., 2013, Tectonic evolution and mantle structure of the Caribbean: *Journal of Geophysical Research: Solid Earth*, v. 118, p. 3019–3036, <https://doi.org/10.1002/jgrb.50235>.
- Walker, J.A., Carr, M.J., Patino, L.C., Johnson, C.M., Feigenson, M.D., and Ward, R.L., 1995, Abrupt change in magma generation processes across the Central American arc in southeastern Guatemala: *Flux-dominated melting near the base of the wedge to decompression melting near the top of the wedge: Contributions to Mineralogy and Petrology*, v. 120, p. 378–390, <https://doi.org/10.1007/BF00306515>.
- Walker, J.A., Patino, L.C., Cameron, B.I., and Carr, M.J., 2000, Petrogenetic insights provided by compositional transects across the Central American arc: Southeastern Guatemala and Honduras: *Journal of Geophysical Research: Solid Earth*, v. 105, p. 18,949–18,963, <https://doi.org/10.1029/2000JB900173>.
- Walker, J.A., Teipel, A.P., Ryan, J.G., and Syracuse, E., 2009, Light elements and Li isotopes across the northern portion of the Central American subduction zone: *Geochemistry, Geophysics, Geosystems*, v. 10, Q06S16, <https://doi.org/10.1029/2009GC002414>.
- Zhou, Q., Hu, J., Liu, L., Chaparro, T., Stegman, D.R., and Faccenda, M., 2018, Western U.S. seismic anisotropy revealing complex mantle dynamics: *Earth and Planetary Science Letters*, v. 500, p. 156–167, <https://doi.org/10.1016/j.epsl.2018.08.015>.
- Zhu, H., Stern, R.J., and Yang, J., 2020, Seismic evidence for subduction-induced mantle flows underneath Middle America: *Nature Communications*, v. 11, 2075, <https://doi.org/10.1038/s41467-020-15492-6>.

Printed in the USA